

Dosimetric Effect of Cobalt-Chrome Stabilization Hardware in Paraspinal Radiation Treatments

Grace Tang¹, Thomas LoSasso¹, Seng-Boh Lim¹, Yoshiya Yamada²,
Mark Bilsky³, Dale Michael Lovelock¹

¹Department of Medical Physics, Memorial Sloan Kettering Cancer Center, New York, USA

²Department of Radiation Oncology, Memorial Sloan Kettering Cancer Center, New York, USA

³Department of Neurosurgery, Memorial Sloan Kettering Cancer Center, New York, USA

Email: tangg@mskcc.org

How to cite this paper: Tang, G., LoSasso, T., Lim, S.-B., Yamada, Y., Bilsky, M. and Lovelock, D.M. (2022) Dosimetric Effect of Cobalt-Chrome Stabilization Hardware in Paraspinal Radiation Treatments. *International Journal of Medical Physics, Clinical Engineering and Radiation Oncology*, 11, 176-187.

<https://doi.org/10.4236/ijmpcero.2022.113015>

Received: July 22, 2022

Accepted: August 28, 2022

Published: August 31, 2022

Copyright © 2022 by author(s) and Scientific Research Publishing Inc. This work is licensed under the Creative Commons Attribution International License (CC BY 4.0).

<http://creativecommons.org/licenses/by/4.0/>



Open Access

Abstract

High density materials are assigned with an apparent density of 3.2 g/cm³ in 12-bit CT images due to saturation. This is often ignored in planning for spine tumors with titanium (density 4.40 g/cm³) spinal hardware. However, new cobalt-chrome hardware has a density of 8.11 g/cm³, which would increase dosimetric uncertainty if the true density is not utilized in planning. This effect was evaluated in this study. Calculation accuracy was examined using MapCHECK2 with a single 20 × 10 cm² field with a titanium and a cobalt-chrome rod in a solid water phantom for 6X, 6FFF and 15X, at 2 cm and 6 cm beneath the rods. Measurement was compared to the calculation with density override (DO) with the true density and to the calculation with no-density override (NDO). Additionally, the dosimetric effect in clinical treatment plans was investigated for six IMRT and VMAT paraspinal cases. Plan quality was compared with the original NDO calculation and the DO recalculation. Compared to measurements, the treatment planning system (TPS) overestimated the dose locally by up to 13.2% for cobalt-chrome and 4.8% for titanium with NDO calculations. DO calculations improved the differences to 8.4% and 4.0%, respectively. Scatter from the rod increased the lateral dose and diminished as depth increased but was not properly accounted for by the TPS even with the correct density assigned. For the clinical plans, PTV coverage was lowered by an average of ~1.0% (range: 0.5% - 2.0%) and ~0.3% (range: 0.2% - 0.7%) in DO recalculations for cobalt-chrome and titanium, respectively. In conclusion, neglecting the true density of cobalt-chrome hardware during planning may result in an unexpected decrease in target coverage.

Keywords

Cobalt-Chrome, Spinal Hardware, Paraspinal Radiation Therapy

1. Introduction

Metallic implants consisting of screw-rod systems are frequently used to reconstruct and stabilize the spine following resection of metastatic and primary spinal tumor. As the life expectancy of these patients has improved due to advances in systematic and radiation therapy [1], an increased number of symptomatic implant failures, specifically rod fractures, have been diagnosed requiring complicated revision surgery. The durability of spinal implants is dependent on achieving arthrodesis, which is difficult in heavily irradiated bone [2]. To reduce the risk of rod fracture in spine-tumor reconstruction, a more durable rod material is needed [3] [4] [5] [6] [7]. The most commonly used spinal stabilization hardware is made of titanium, while new hardware systems have emerged in recent years including those made with carbon-fiber-reinforced polyetheretherketone (CFR-PEEK) and cobalt-chrome. Compared to titanium, cobalt-chrome is a stronger material with a higher physical density ($\sim 8.11 \text{ g/cm}^3$ for cobalt-chrome and $\sim 4.40 \text{ g/cm}^3$ for titanium). With 12-bit CT, the apparent density of these high-density materials is approximately 3.2 g/cm^3 due to Hounsfield Units (HU) saturation at around 3095. Without assigning the true density to these materials, dosimetric uncertainties may be introduced to the treatment plan. On the other hand, it can be a tedious process to contour the spinal fixation hardware and override the density. Therefore, it is not uncommon to calculate the dose for paraspinal cases without overriding the true density of the standard titanium hardware in clinical practice. However, the underestimation of density due to the saturation of HU is larger for cobalt-chrome and the dosimetric uncertainty may be amplified. While the dosimetric effect of titanium hardware has been widely studied [8]-[14], to our best knowledge, this is the first study to evaluate the dosimetric effect of cobalt-chrome spinal hardware for single fraction and hypofractionated paraspinal IMRT and VMAT cases. Data is presented to support a clinical decision on the necessity to contour the hardware and assign the correct electron density for treatment planning.

2. Methods and Materials

2.1. Accuracy of Dose Calculation with Spinal Hardware

Dose calculation accuracy with the presence of titanium and cobalt-chrome was verified with measurement using the MapCHECK[®]2 (Sun Nuclear, Melbourne, FL). A titanium rod and a cobalt-chrome rod were taken out of the spinal fixation systems (Symphony[™] OCT System, DePuy Synthes, Rayndam, MA) and were machined to embed in a solid water cuboid for easy measurement setup. The hardware cuboids were placed on a stack of $30 \times 30 \text{ cm}^2$ solid water slabs for measurement, with the center of the rods at 2.5 cm below surface. The inherent spatial resolution of MapCHECK2 is approximately 7 mm while the titanium and cobalt-chrome rods are approximately 6.4 mm in diameter. Therefore, the MapCHECK2 was shifted incrementally to achieve a measurement resolution of 1 mm. For a single open field with a field size of $20 \times 10 \text{ cm}^2$, MapCHECK2 mea-

surement was done at 2 cm and 6 cm below the center of the rods for 6X and 15X beams. For 6FFF beam, a field size of $15 \times 10 \text{ cm}^2$ was used for measurement due to beam model limitations in the treatment planning system. The measured beam profiles were symmetrized based on the average values of both sides to eradicate rod positioning error. To eliminate the effect of daily linac output fluctuation for comparison, the CAX dose from an open field measurement (without rods) was normalized to the same point in dose calculation for all energies. Dose calculation was done with Eclipse v13.6 (Varian Medical Systems, Palo Alto, CA) using the AAA algorithm with 1 mm dose grid. The CT image-set used for calculation was based on a virtual phantom that simulates the measurement setup. The rods in the CT (Brilliance Big Bore, Philips Medical Systems, Cleveland, USA) were assigned with 3095 HU, which was the saturated HU value, and the corresponding calculation was identified as no-density override (NDO). Another set of calculations was done with assigning the true density, which was achieved by extrapolating the existing 12-bit CT calibration curve. The titanium and cobalt-chrome rods were assigned with 4782 HU and 10,549 HU, which corresponded to a density of 4.40 and 8.11 g/cm^3 . The set of calculations done with the correct density was identified as density override (DO) calculations.

2.2. Dosimetric Effects on Plan Quality

A total of six paraspinal cases, including five VMAT and one IMRT, from five different patients were randomly selected for a retrospective study. All patients have titanium spinal hardware in the proximity of the target. The disease location and the prescription information are tabulated in **Table 1**. The spinal hardware structures in the CT images were contoured so that the true density could be assigned manually. The rods and screws of the hardware were contoured separately. The titanium hardware set comprised both titanium rods and titanium screws, whereas the cobalt-chrome hardware set comprised of cobalt-chrome rods and titanium screws. It is worth noting that the construction of the titanium hardware and cobalt-chrome hardware is identical, with only a difference in rod material in the hardware system. The original clinical treatment plan was calculated without proper density assignment to the metallic structures,

Table 1. Patient information with disease location and prescription.

Patient	Disease	Prescription	Plan
1	T9 - T12	6 Gy \times 5	VMAT
2	T4 - T5	8 Gy \times 5	VMAT
3	T10 - T12	24 Gy \times 1	VMAT
4	T5	24 Gy \times 1	VMAT
4	T8	24 Gy \times 1	VMAT
5	T9	24 Gy \times 1	IMRT

based on a density of 3.2 g/cm^3 and 3095 HU (*i.e.*, NDO). Two other sets of calculations of the same plan were done by assigning the hardware with 4782 HU and 10,549 HU, which correspond to a density of 4.40 and 8.11 g/cm^3 for titanium and cobalt-chrome, respectively. The plan quality of these plans was compared to the original NDO plan where the hardware had no density-override.

3. Results

3.1. Calculation Accuracy with Single Open Field

The comparison between MapCHECK2 measurements and calculations is summarized in **Figure 1** and **Table 2**. For a single open field, AAA underestimated the attenuation and lateral scatter of the rods compared to measurement. This effect was more prominent for cobalt-chrome compared to titanium. At 2 cm below the rods, without overriding with the true density, the ratio of NDO calculation and measurement was 1.131 for cobalt-chrome and 1.044 for titanium for 6X. The corresponding mean dose ratio within a 4 cm ROI (± 2 cm around the central axis of the rod) was 1.010 and 0.997 for cobalt-chrome and titanium rods, respectively. Dose calculation accuracy was increased by assigning the true density, where the point dose ratio decreased to 1.084 for cobalt-chrome and 1.036 for titanium, while the mean dose ratios were similar, 0.999 and 0.995, for cobalt-chrome and titanium rods, respectively. The minimal improvement in DO calculation for titanium was expected considering the misrepresentation for titanium was 3.2 g/cm^3 (3095 HU) in NDO calculation instead of 4.4 g/cm^3 (4782 HU) in DO calculation. However, the difference in erroneous density assignment for cobalt-chrome was much larger, where the true value was 8.11 g/cm^3 . This resulted in a greater difference between NDO and DO calculations for cobalt-chrome. The results of the 6FFF beam were very similar to 6X since the energy was also very similar. For 15X, the point dose ratio was 1.095 and 1.033 and the mean dose ratio was 1.009 and 1.000 for cobalt-chrome and titanium rods, respectively, when comparing measurement to NDO calculation. With DO calculation, the point dose ratio to measurement improved to 1.064 and 1.028, and the mean dose ratio was 1.001 and 0.998 for cobalt-chrome and titanium rods, respectively.

Even with the true density assigned in calculation, AAA was not able to account for the presence of high density material properly. The magnitude of the dosimetric discrepancies between calculation and measurement was consistent at a deeper depth, where the dose ratios at 2 cm and 6 cm below rods were within 0.8% for both rods and all energies. The local dose differences within ± 2 cm from the central axis of the rod suffer from the underestimation of lateral scatter due to the limitation of “modified” pencil beam kernel used in the AAA algorithm [15] [16] [17]. This was more apparent at 2 cm below the rod than at 6 cm as shown in **Figure 2(b)** and **Figure 2(d)**, as the lateral scatter contribution from the rod diminished at a deeper depth. This effect was more prominent for cobalt-chrome (*i.e.*, material with higher density) and 6X and 6FFF beams (*i.e.*, lower

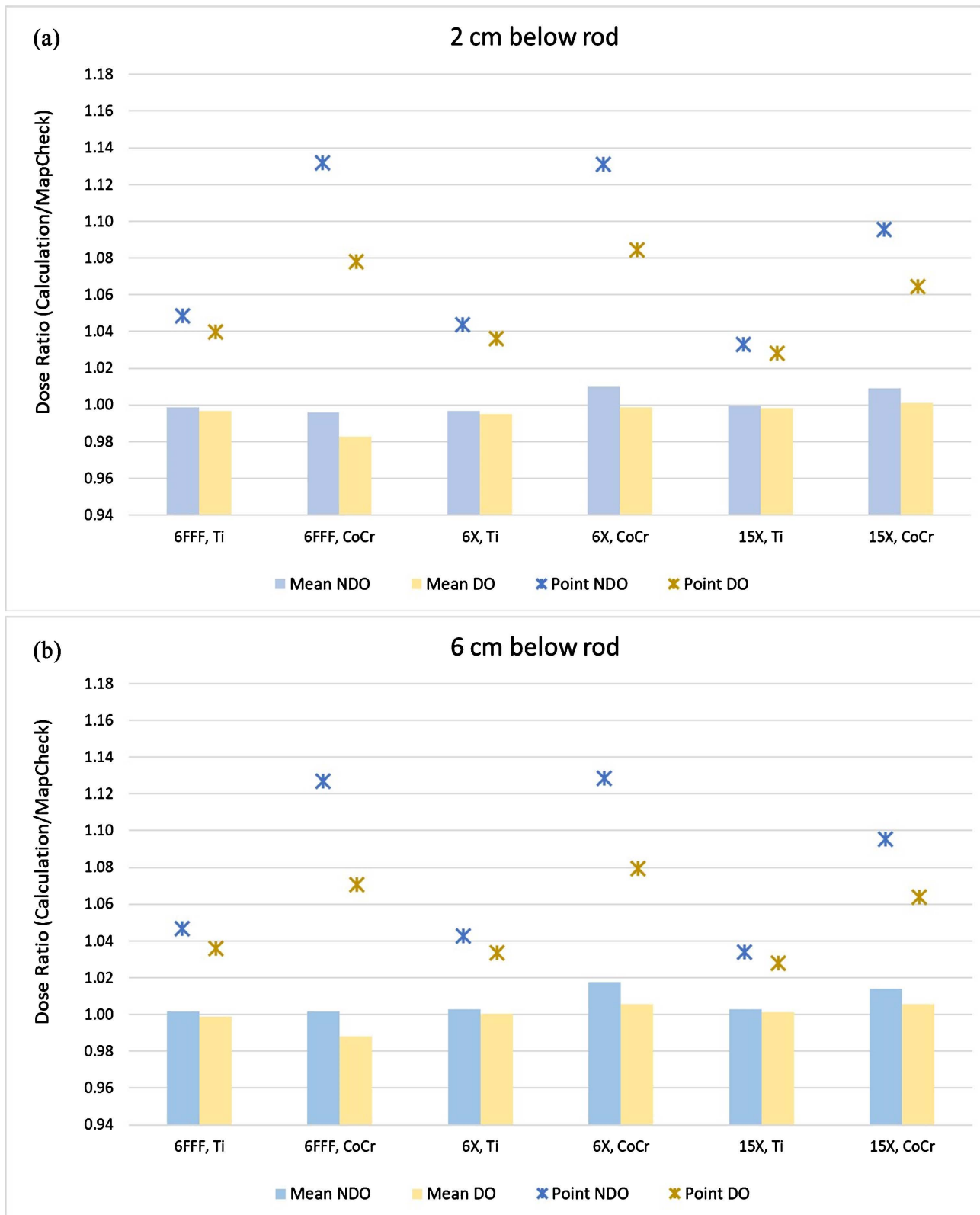


Figure 1. Ratio of dose calculation and MapCHECK2 measurement, with and without density override (DO and NDO) for a single open field with titanium and cobalt-chrome rods at (a) 2 cm below rod and (b) 6 cm below rod. The mean dose ratio was defined as the average dose ratio within a ROI ± 2 cm about the central axis of the rod and the point dose ratio was the dose ratio at the central axis of the rod.

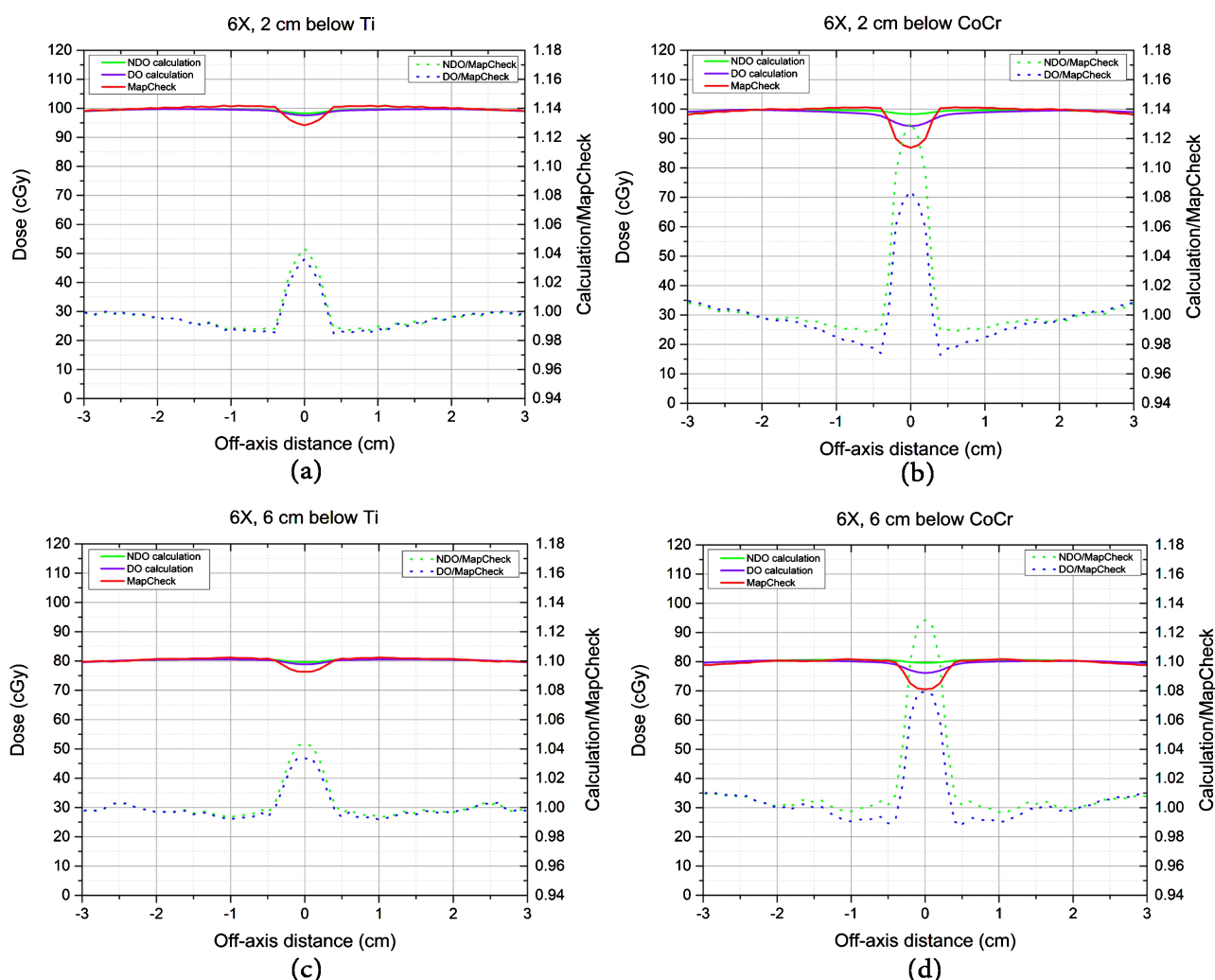


Figure 2. Profile comparison between calculations and measurements, with and without density override (*i.e.* DO and NDO), for a single open field exposed to (a) a titanium rod and (b) a cobalt-chrome rod, at 2 cm below the rods; and (c) and (d) are the profiles at 6 cm below the titanium rod and cobalt-chrome rod, respectively. The ratios between calculations and measurements are plotted in dotted lines.

Table 2. Dose ratios between calculations and MapCHECK2 measurement for a single open field with titanium and cobalt-chrome rods (calculation/measurement). The point dose ratio was the dose ratio at the central axis of the rod and the mean dose ratio was defined as the average dose ratio within a ROI ± 2 cm about the central axis of the rod.

Beam	Rod	2 cm below rod				6 cm below rod			
		NDO calculation/M		DO calculation/M		NDO calculation/M		DO calculation/M	
		Point	Mean	Point	Mean	Point	Mean	Point	Mean
6FFF	Ti	1.048	0.999	1.040	0.997	1.047	1.002	1.036	0.999
	CoCr	1.132	0.996	1.078	0.983	1.127	1.002	1.071	0.988
6X	Ti	1.044	0.997	1.036	0.995	1.043	1.003	1.033	1.000
	CoCr	1.131	1.010	1.084	0.999	1.129	1.018	1.080	1.006
15X	Ti	1.033	1.000	1.028	0.998	1.034	1.003	1.028	1.001
	CoCr	1.095	1.009	1.064	1.001	1.095	1.014	1.064	1.006

energy). Although the shape of the dose distribution below the rod was not accurately modeled by AAA, the integral dose was consistent for all energies and all depths based on the mean dose ratios of 0.997 on average for cobalt-chrome (range: 0.983 - 1.006) and 0.998 on average for titanium (range: 0.995 - 1.001), when comparing DO calculation to measurement.

3.2. Dosimetric Impact on Clinical Cases

The local dose differences observed in the single field measurements were diminished for clinical IMRT and VMAT plans, where beams were oriented in multiple directions. In general, there was an overall decrease in dose in DO recalculations as expected for the six paraspinal cases (see **Table 3**). Due to the larger relative difference in apparent density (in original NDO calculation) and true density (in DO recalculation), a greater difference in dose was seen in the DO recalculation for cobalt-chrome than for titanium as demonstrated in **Figure 3**. Recalculation

Table 3. Difference between recalculation (DO) and original calculation (NDO) for six paraspinal cases.

Patient	ROI	Metric	Recalculation (DO) - Original (NDO) calculation	
			Titanium	Cobalt-chrome
1	PTV	V95%	-0.2%	-0.9%
		Max	-0.8%	-1.8%
	Cord	Max	-18.3 cGy	-24.7 cGy
	Cauda	Max	-8.4 cGy	-12.0 cGy
	Bowel	Max	-2.0 cGy	-7.1 cGy
2	PTV	V95%	-0.2%	-0.5%
		Max	-0.2%	-0.9%
	Cord	Max	2.4 cGy	5.8 cGy
	Lt brachial plexus	Max	-3.3 cGy	-7.2 cGy
	Rt brachial plexus	Max	-1.6 cGy	-3.9 cGy
3	PTV	V95%	-0.2%	-0.5%
		Max	0.0%	0.0%
	Cord	Max	2.0 cGy	-12.7 cGy
	Bowel	Max	-31.1 cGy	-33.0 cGy
	Stomach	Max	-1.2 cGy	-4.7 cGy
4 (T5)	PTV	V95%	-0.6%	-1.0%
		Max	-2.2%	-2.4%
	Cord	Max	-6.9 cGy	-16.3 cGy
	Esophagus	V18Gy	-0.2 cc	-0.3 cc

Continued

4(T8)	PTV	V95%	-0.2%	-0.9%
		Max	0.4%	-0.3%
	Cord	Max	-6.0 cGy	-22.1 cGy
		Heart	Max	-6.2 cGy
			D15cc	-4.6 cGy
	Esophagus	V18Gy	-0.1 cc	-0.2 cc
5	PTV	V95%	-0.7%	-2.0%
		Max	-0.5%	-1.3%
	Cord	Max	-6.3 cGy	-22.1 cGy

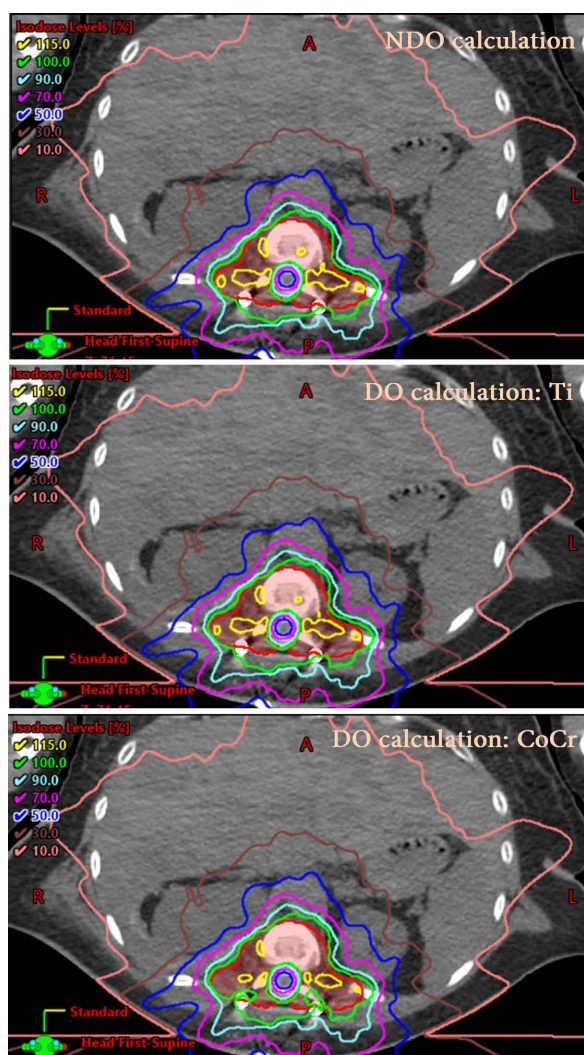


Figure 3. Isodose distributions of NDO calculation, DO calculation for titanium hardware, and DO calculation for cobalt-chrome hardware for Patient 1. PTV is depicted with the red contour. PTV coverage is slightly degraded with the DO calculation for cobalt chrome hardware as shown by the 100% isodose line (green) compared to the NDO calculation and the DO calculation for titanium hardware.

with DO minimally lowered the PTV coverage (V95%) by an average of ~0.3% (range: 0.2% - 0.7%) and ~1.0% (range: 0.5% - 2.0%) for titanium and cobalt-chrome, respectively. For Patient 2, the slight increase in maximum cord dose in DO recalculations of both rod materials may be due to the proximity of the screws to the cord. Similarly, for Patient 3, the maximum cord dose was minimally higher in the titanium recalculation as the cord was in close proximity to the screws. However, the effect of the increased lateral scatter from the titanium screws was diminished compared to the high attenuation of the cobalt-chrome rods. This was not observed in Patient 2 because the plan consisted of 2 full rotational arcs while the plan for Patient 3 consisted of 6 partial posterior arcs.

4. Discussion

In general, contouring the spinal hardware and overriding the density is not part of the standard planning process in our clinic. The concern in dosimetric uncertainty may not be prominent based on the density of titanium, which is the standard material used in spinal support hardware. However, this may no longer be true for cobalt-chrome rods, which emerged as a new and sturdier spinal hardware, with a higher density than titanium (8.11 g/cm³ vs. 4.40 g/cm³). The dosimetric uncertainty mainly arises from two factors: 1) erroneous assignment of HU due to the limitation of 12-bit CT, and 2) dose calculation inaccuracy with high density materials. The HU assignment problem may be resolved by an extended CT curve or a 16-bit CT [18] [19] but it should be cautioned that the resultant electron density should be verified. At the end of this study, all CT scanners at our institution were upgraded to be 16-bit. The CT calibration curve was reacquired using a CT calibration phantom with titanium and stainless inserts. With 10 different CT units in our network, a remarkable variation in HU of these high density materials was observed although all units were configured with the same kVp (*i.e.*, 120 kV) and similar mAs settings. For example, one scanner determined the titanium rod to have a HU of 7360, which corresponded to a relative electron density of 5.4 but the true electron density of titanium is 3.8. For cobalt-chrome rod, the HU was 16,669, which corresponded to a relative electron density of 12.8 while the true value should be 7.3. These large discrepancies warrant density override. The variation in HU for high density material is not yet fully understood and is under active investigation. A possible alternative solution would be dual-energy CT, which has been proven to reduce metal artifacts and quantify the material property more accurately [20] [21] [22].

The second culprit of dosimetric uncertainty in calculating with metallic objects is inherent in the limitation of the calculation algorithm in the treatment planning system. While it has been widely established that Monte Carlo algorithms can best estimate the dose distributions with the presence of metallic implants [9] [11] [23] [24], dose calculation with high density materials is not accurate with the AAA algorithm. As demonstrated from the open beam measurements in **Figure 2**, AAA underestimated the lateral scatter and attenuation

of titanium and cobalt-chrome, and the inaccuracy increased with material density. This is consistent with the findings of Lloyd and Ansbacher [25], where they observed inaccuracy in both lateral scatter and attenuation in AAA calculations with stainless steel, which has a similar density to cobalt-chrome.

As expected, based on the results in **Figure 1**, the dosimetric uncertainty for 15X is less compared to the lower energy beams but 6X and 6FFF are the typical energy choices for paraspinal treatment. Using preferential beam angle is a good solution where beam entries are avoided and is often adopted in pelvic cases with hip prosthesis [26] [27] [28] but this is limited for paraspinal cases as posterior beams are preferred. Another option is to assign the spinal hardware as “avoidance structures”, which can further limit beam entrance/exit during optimization (note that this option might not be available in some treatment planning systems). Nonetheless, for the six patient cases in this study, the dosimetric impact was diminished in IMRT/VMAT plans with multiple beams, *i.e.*, the average difference between NDO calculations and DO calculations was within 1% in target coverage for cases with cobalt-chrome hardware. On the other hand, the optimization algorithm is capable of handling high-density materials if DO is utilized. Individual clinics should weigh the clinical significance of these dosimetric uncertainties, and the additional time taken to contour and reassign the support hardware with the true density for any changes in practice.

5. Conclusion

In addition to the intrinsic limitation in dose calculation accuracy in the treatment planning system, dosimetric uncertainty is increased with cobalt-chrome spinal hardware, especially when the incorrect HU value is assigned due to CT saturation. This may lead to an unexpected decrease in target coverage if proper care is not taken.

Conflicts of Interest

The authors declare no conflicts of interest regarding the publication of this paper.

References

- [1] Anick Nater, A.S. and Fehlings, M. (2018) Chapter 16. Management—Spinal Metastases. In: Schiff, D. and van den Bent, M.J., Eds., *Handbook of Clinical Neurology*, Vol. 149, Elsevier, Amsterdam, 239-255.
<https://doi.org/10.1016/B978-0-12-811161-1.00016-5>
- [2] Park, S.-J., Lee, C.-S., Chang, B.-S., Kim, Y.-H., Kim, H., Kim, S.-I. and Chang, S.-Y. (2019) Rod Fracture and Related Factors after Total en Bloc Spondylectomy. *The Spine Journal*, **19**, 1613-1619. <https://doi.org/10.1016/j.spinee.2019.04.018>
- [3] Shah, K.N., Walker, G., Koruprolu, S.C. and Daniels, A.H. (2018) Biomechanical Comparison between Titanium and Cobalt Chromium Rods Used in a Pedicle Subtraction Osteotomy Model. *Orthopedic Reviews*, **10**, 7541-7541.
<https://doi.org/10.4081/or.2018.7541>

- [4] Yamanaka, K., Mori, M., Yamazaki, K., Kumagai, R., Doita, M. and Chiba, A. (2015) Analysis of the Fracture Mechanism of Ti-6Al-4V Alloy Rods That Failed Clinically after Spinal Instrumentation Surgery. *Spine*, **40**, E767-E773. <https://doi.org/10.1097/BRS.0000000000000881>
- [5] Li, C.S., Vannabouathong, C., Sprague, S. and Bhandari, M. (2015) The Use of Carbon-Fiber-Reinforced (CFR) PEEK Material in Orthopedic Implants: A Systematic Review. *Clinical Medicine Insights. Arthritis and Musculoskeletal Disorders*, **23**, 33-45. <https://doi.org/10.4137/CMAMD.S20354>
- [6] Müller, B., Ryang, Y.M., Oechsner, M., Düsberg, M., Meyer, B., Combs, S.E. and Wilkens, J.J. (2020) The Dosimetric Impact of Stabilizing Spinal Implants in Radiotherapy Treatment Planning with Protons and Photons: Standard Titanium Alloy vs. Radiolucent Carbon Fiber-Reinforced PEEK Systems. *Journal of Applied Clinical Medical Physics*, **21**, 6-14. <https://doi.org/10.1002/acm2.12905>
- [7] Shi, C., Lin, H., Huang, S., Xiong, W., Hu, L., Choi, I., Press, R., Hasan, S., Simone, C. and Chhabra, A. (2022) Comprehensive Evaluation of Carbon-Fiber-Reinforced Polyetheretherketone (CFR-PEEK) Spinal Hardware for Proton and Photon Planning. *Technology in Cancer Research and Treatment*, **21**, 1-11. <https://doi.org/10.1177/15330338221091700>
- [8] Liebross, R.H., Starkschall, G., Wong, P.F., Horton, J., Gokaslan, Z.L. and Komaki, R. (2002) The Effect of Titanium Stabilization Rods on Spinal Cord Radiation Dose. *Medical Dosimetry*, **27**, 21-24. [https://doi.org/10.1016/S0958-3947\(02\)00083-3](https://doi.org/10.1016/S0958-3947(02)00083-3)
- [9] Mesbahi, A. and Nejad, F.S. (2007) Monte Carlo Study on the Impact of Spinal Fixation Rods on Dose Distribution in Photon Beams. *Reports of Practical Oncology and Radiotherapy*, **12**, 261-266. [https://doi.org/10.1016/S1507-1367\(10\)60064-8](https://doi.org/10.1016/S1507-1367(10)60064-8)
- [10] Son, S.H., Kang, Y.N. and Ryu, M.R. (2012) The Effect of Metallic Implants on Radiation Therapy in Spinal Tumor Patients with Metallic Spinal Implants. *Medical Dosimetry*, **37**, 98-107. <https://doi.org/10.1016/j.meddos.2011.01.007>
- [11] Wang, X., Yang, J.N., Li, X., Tailor, R., Vassilliev, O., Brown, P., Rhines, L. and Chang, E. (2013) Effect of Spine Hardware on Small Spinal Stereotactic Radiosurgery Dosimetry. *Physics in Medicine and Biology*, **58**, 6733-6747. <https://doi.org/10.1088/0031-9155/58/19/6733>
- [12] Li, J., Yan, L., Wang, J., Cai, L. and Hu, D. (2015) Influence of Internal Fixation Systems on Radiation Therapy for Spinal Tumor. *Journal of Applied Clinical Medical Physics*, **16**, 279-289. <https://doi.org/10.1120/jacmp.v16i4.5450>
- [13] Yazici, G., Sari, S.Y., Yedekci, F.Y., Yucekul, A., Birgi, S.D., Demirkiran, G., Gultekin, M., Hurmuz, P., Yazici, M., Ozyigit, G. and Cengiz, M. (2016) The Dosimetric Impact of Implants on the Spinal Cord Dose during Stereotactic Body Radiotherapy. *Radiation Oncology*, **11**, Article No. 71. <https://doi.org/10.1186/s13014-016-0649-z>
- [14] Cheng, Z.J., Bromley, R.M., Oborn, B., Carolan, M. and Booth, J.T. (2016) On the Accuracy of Dose Prediction near Metal Fixation Devices for Spine SBRT. *Journal of Applied Clinical Medical Physics*, **17**, 475-485. <https://doi.org/10.1120/jacmp.v17i3.5536>
- [15] Ulmer, W. and Harder, D. (1995) A Triple Gaussian Pencil Beam Model for Photon Beam Treatment Planning. *Zeitschrift für Medizinische Physik*, **5**, 25-30. [https://doi.org/10.1016/S0939-3889\(15\)70758-0](https://doi.org/10.1016/S0939-3889(15)70758-0)
- [16] Ulmer, W. and Harder, D. (1996) Applications of a Triple Gaussian Pencil Beam Model for Photon Beam Treatment Planning. *Zeitschrift für Medizinische Physik*,

- 6, 68-74. [https://doi.org/10.1016/S0939-3889\(15\)70784-1](https://doi.org/10.1016/S0939-3889(15)70784-1)
- [17] Sievinen, J., Ulmer, W. and Kaissl, W. (2005) AAA Photon Dose Calculation in Eclipse. Varian Documentation RAD #7170B.
- [18] Glide-Hurst, C., Chen, D., Zhong, H. and Chetty, I.J. (2013) Changes Realized from Extended Bit-Depth and Metal Artifact Reduction in CT. *Medical Physics*, **40**, Article ID: 061711. <https://doi.org/10.1118/1.4805102>
- [19] Mullins, J.P., Grams, M.P., Herman, M.G., Brinkmann, D.H. and Antolak, J.A. (2016) Treatment Planning for Metals Using an Extended CT Number Scale. *Journal of Applied Clinical Medical Physics*, **17**, 179-188. <https://doi.org/10.1120/jacmp.v17i6.6153>
- [20] Guggenberger, R., Winklhofer, S., Osterhoff, G., Wanner, G.A., Fortunati, M. and dreisek, G., Alkadhi, H. and Stolzmann, P. (2021) Metallic Artefact Reduction with Monoenergetic Dual-Energy CT: Systematic *ex Vivo* Evaluation of Posterior Spinal Fusion Implants from Various Vendors and Different Spine Levels. *European Radiology*, **22**, 2357-2364. <https://doi.org/10.1007/s00330-012-2501-7>
- [21] Pessis, E., Sverzut, J.M., Campagna, R., Guerini, H., Feydy, A. and Drapé, J.L. (2015) Reduction of Metal Artifact with Dual-Energy CT: Virtual Monospectral Imaging with Fast Kilovoltage Switching and Metal Artifact Reduction Software. *Seminars in Musculoskeletal Radiology*, **19**, 446-455. <https://doi.org/10.1055/s-0035-1569256>
- [22] Pettersson, E., Bäck, A. and Thilander-Klang, A. (2021) Comparison of Metal Artefacts for Different Dual Energy CT Techniques. *Radiation Protection Dosimetry*, **195**, 232-245. <https://doi.org/10.1093/rpd/ncab105>
- [23] Wieslander, E. and Knöös, T. (2003) Dose Perturbation in the Presence of Metallic Implants: Treatment Planning System versus Monte Carlo Simulations. *Physics in Medicine and Biology*, **48**, 3295-3305. <https://doi.org/10.1088/0031-9155/48/20/003>
- [24] Spadea, M.F., Verburg, J.M., Baroni, G. and Seco, J. (2014) The Impact of Low-Z and High-Z Metal Implants in IMRT: A Monte Carlo Study of Dose Inaccuracies in Commercial Dose Algorithms. *Medical Physics*, **41**, Article ID: 011702. <https://doi.org/10.1118/1.4829505>
- [25] Lloyd, S.A.M. and Ansbacher, W. (2013) Evaluation of an Analytic Linear Boltzmann Transport Equation Solver for High-Density in Homogeneities. *Medical Physics*, **40**, Article ID: 011707. <https://doi.org/10.1118/1.4769419>
- [26] Keall, P.J., Siebers, J.V., Jeraj, R. and Mohan, R. (2003) Radiotherapy Dose Calculations in the Presence of Hip Prostheses. *Medical Dosimetry*, **28**, 107-112. [https://doi.org/10.1016/S0958-3947\(02\)00245-5](https://doi.org/10.1016/S0958-3947(02)00245-5)
- [27] Reft, C., Alecu, R., Das, I.J., Gerbi, B.J., Keall, P., Lief, E., Mijnheer, B.J., Papanicolaou, N., Sibata, C. and Van Dyk, J. (2003) Dosimetric Considerations for Patients with HIP Prostheses Undergoing Pelvic Irradiation. Report of the AAPM Radiation Therapy Committee Task Group 63. *Medical Physics*, **30**, 1162-1182. <https://doi.org/10.1118/1.1565113>
- [28] Prabhakar, R., Kumar, M., Cheruliyil, S., Jayakumar, S., Balasubramanian, S. and Cramb, J. (2013) Volumetric Modulated Arc Therapy for Prostate Cancer Patients with Hip Prosthesis. *Reports of Practical Oncology and Radiotherapy*, **18**, 209-213. <https://doi.org/10.1016/j.rpor.2013.03.006>